Capture-aware identification of mobile RFID tags with unreliable channels

Article (Accepted Version)

Capture-aware Identification of Mobile RFID Tags with Unreliable Channels

Jian Su, *Member, IEEE*, Zhengguo Sheng, *Senior Member, IEEE*, Alex. X. Liu, *Fellow, IEEE*, Yu Han, *Member, IEEE*, and Yongrui Chen, *Member, IEEE*

Abstract—Radio frequency identification (RFID) has been widely applied in large-scale applications such as logistics, merchandise and transportation. However, it is still a technical challenge to effectively estimate the number of tags in complex mobile environments. Most of existing tag identification protocols assume that readers and tags remain stationary throughout the whole identification process and ideal channel assumptions are typically considered between them. Hence, conventional algorithms may fail in mobile scenarios with unreliable channels. In this paper, we propose a novel RFID anti-collision algorithm for tag identification considering path loss. Based on a probabilistic identification model, we derive the collision, empty and success probabilities in a mobile RFID environment, which will be used to define the cardinality estimation method and the optimal frame length. Both simulation and experimental results of the proposed solution show noticeable performance improvement over the commercial solutions.

Index Terms—RFID, anti-collision, propagation, unreliable channel, time efficiency.

1 Introduction

As a non-contact communication technology that uses RF signals and spatially coupled transmission to automatically identify objects, RFID significantly contributes to the large-scale deployment of Internet-of-Things (IoT) [1-2]. For example in applications, such as warehouse, baggage sorting, retail distribution and intelligent transportation [3-5], a large number of items are placed on a moving conveyor, cart and need to be managed accordingly. To improve the efficiency of management and optimize the supply chain in such applications, mobile RFID tags (i.e., attached to moving items) need to be identified efficiently to allow manufacturers to obtain accurate and timely stock information.

Because the communication between a reader and tags shares a same wireless channel, co-channel interference may happen when multiple tags respond to the reader simultaneously, which results in a multi-tag collision phenomenon and leads to reduced identification efficiency, increased misreading rate and identification latency, hence limits the reading performance of RFID tags in large scales [6]. In addition, physical layer factors, such as path loss and signal attenuation, change over time in mobile RFID scenarios, which further hinders the data exchange between the reader and tags and leads to increased tag misreading. In mobile scenarios, even a slot is occupied by only one tag, the reader may fail to identify it due to the unreliability of channel conditions. In this case, ensuring a reliable reading performance of mobile RFID becomes very challenging. Thus, we need to explore anti-collision algorithms for mobile RFID scenarios.

Due to the attribute of low energy and computing power, RFID tags can not self-regulate their radio transmission to avoid collisions. Collision avoidance communications of RFID system are mainly realized by adopting anti-collision mechanisms and algorithms on the reader side. The purpose of an anti-collision algorithm is to obtain the IDs of all available tags within minimal time. At present, there are two mainstream anti-collision algorithms, namely Aloha-based [6-9] algorithms and tree-based [10-14] algorithms (including Query tree [10-12] and tree splitting [13-14]). Among them, the Aloha-based method is more favorable by EPC C1 Gen2 UHF RFID standard. Most RFID manufacturers currently comply with the EPC C1 Gen2 standard and promote Aloha-based algorithm applications. Existing anti-collision algorithms focus on parameters optimization for identifying stationary RFID tags under an ideal channel condition [6-9]. Thus, they are difficult to adapt to complex mobile environments due to the following reasons. For tree-based algorithms, the recursive splitting procedure assumes an unchanged tag cardinality. However, in a mobile environment, the number of tags involved in splitting procedure may change over time, which causes a large number of tag missing. For Aloha-based algorithms, the conventional cardinality estimation and its optimal frame setting will also become inapplicable due to the tag mobility and changes in statistical characteristics. Although some works [15-17] attempt to optimize the parameters through experiments, their findings are unable to apply to general settings in mobile environments.

In this paper, to tackle the above challenges in mobile tag identification, we investigate effective approaches to improve reading performance for a large volume of tags under mobile environment with unreliable channel conditions.

J. Su is with the School of Computer and Software, Nanjing University of Information Science and Technology, Jiangsu 210044, China (e-mail: sj890718@gmail.com).
Z. Sheng is with the Department of Engineering and Design, University of Sussex, Brighton BN1 9RH, U.K. (e-mail: z.sheng@sussex.ac.uk).
A. X. Liu is with the Department of Computer Science and Engineering, Michigan State University, East Lansing, MI 48824 USA (Email: alexliu@cse.msu.edu).
Y. Han is with the School of Information and Communications Engineering, University of Electronic Science and Technology of China, Chengdu 611731, China. (Email: yuhan.uestc@outlook.com).
Y. Chen is with the School of Electronic, Electrical, and Communication Engineering, University of Chinese Academy of Sciences, Beijing, 100190, P.R.China (e-mail: chenyr@ucas.ac.cn).
Digital Object Identifier xxxx

We propose an efficient capture-aware tag identification algorithm (ECATI) to improve the reading performance of mobile RFID tags with unreliable channels. The key idea of ECATI is to transform the mobile tag identification problem into a probabilistic model optimization problem and find the optimal solution that ensures the maximal system efficiency. In ECATI, we first estimate the tag cardinality using an in-frame estimation strategy to reduce the computational complexity. Second, based on the estimated tag cardinality, we calculate the optimal frame length to launch the following identification round so that the expected system efficiency is maximized.

By analyzing the mobility factors, we introduce a probabilistic identification model to characterize the mobile RFID environment. The proposed probabilistic identification model strictly follows the EPC C1 Gen2 UHF RFID standard and provides a fundamental guidance for MAC parameters optimization in mobile RFID tag identification process. Unlike the conventional Aloha-based algorithm, both cardinality estimation and optimal frame setting of ECATI are based on the derivation of collision, empty and success probabilities in a mobile RFID environment. Therefore, when the capture effect and multipath fading occur, the ECATI can adapt to such changes and maintain the reading performance in mobile scenarios.

To evaluate the reading performance of ECATI in a practical mobile RFID environment, we implement ECATI by using a commercial reader manufactured by Impinj Inc and 100 passive RFID tags equipped by Alien Inc. The experiments are carried out by equally spacing RFID tags with 2.5 meters and moving them along a straight trajectory. The evaluation mainly consists of three aspects: 1) the number of identification tags in a given time interval, 2) average identification rate per second, 3) misreading ratio. Experimental results show that the proposed ECATI algorithm improves the average identification rate by 43.4% compared to Impinj R2000 solution.

The remainder of this paper is structured as follows. Section 2 reviews and analyzes the mainstream anti-collision solutions for UHF RFID systems. Section 3 introduces the preliminaries and system model. A novel tag identification algorithm focusing on a mobile environment is presented in Section 4. Section 5 illustrates and discusses the simulation results. The experimental results are presented in Section 6. Finally, the paper is concluded in Section 7.

2 Related Works

With consideration of cost and implementation complexity, the time-division multiple access (TDMA) solutions have been mainly used in RFID systems. That is, each tag occupies the channel in a separated time interval to interact with the reader. TDMA based solutions include Aloha-based algorithms and tree-based algorithms which can be further divided into tree splitting and query tree. Among them, the Aloha-based algorithms are most widely used in UHF RFID and referred by EPC C1 Gen2.

The Aloha-based protocols are firstly developed for random access in packet radio networks. In order to enhance the reading performance of RFID systems, the dynamic framed slotted Aloha (DFSA) is developed and widely used in EPC C1 Gen2 UHF RFID standard. The principle of DFSA algorithm is to divide time into several frame segments, each of which consists of a number of time slots. A tag responds to the reader with its ID when it receives a query command specifying the parameter Q (the number of slots per frame is $F = 2^Q$). The performance of DFSA depends on both the cardinality estimation and setting of the frame length (the number of slots per frame). The slot efficiency is defined as the number of identified tags over the frame length, which is mostly used to evaluate the performance of RFID system. Specifically, the maximum slot efficiency of 0.368 is attained asymptotically when the frame length is equal to the number of tags [18]. To maximize the performance of DFSA, most previous solutions [19-22] require vast computational costs so that the estimation accuracy can be ensured. However, most handheld RFID readers in practice are computation constrained due to their low-cost hardware nature such as a single-core microprocessor.

Recently, some energy-efficient DFSA algorithms have been proposed to lower computational overhead. The literature [23] presents an anti-collision protocol which depends on one examination of frame length at a specific time slot during each identification round. The authors in [24] introduces an Improved Linearized Combinatorial Model (ILCM) to estimate the cardinality with modest calculation cost. However, its performance fluctuates sharply with the number of tags. In [25], the authors presents a FuzzyQ method which integrates fuzzy logic with a DFSA algorithm. A fuzzy rule-based system is defined to model the frame length and collision rate with fuzzy sets to calculate frame length adaptively. However, the performance of FuzzyQ needs to be further improved. In [26], a sub-frame based algorithm (SUBF-DFSA) is proposed to overcome the accumulated estimation error, and hence to improve the performance. Specifically, the tag cardinality is estimated based on the linear relationships between empty and collision slots statistically counted in a sub-frame. Since the computational complexity of the estimation is reduced, the time and energy efficiency of SUBF-DFSA can be improved compared to the estimation methods with high complexity. However, the accuracy of SUBF-DFSA estimation is not sufficient because the usage of empirical correlation is not based on theoretical calculation. The literature [27] proposes a two-phase anti-collision algorithm named detected sector based DFSA (ds-DFSA) to enhance the identification performance. The ds-DFSA algorithm effectively uses empty, singleton and collision statistics in an early observation phase to recursively determine an optimal frame length. After that, the simple calculation is used to estimate the number of concurrent tags contained in each collision slot. And then the reader assigns the individual frame length to resolve each collision slot. However, due to the requirement of new commands, modifications to the existing UHF RFID standard are needed for the ds-DFSA, thus making it difficult to be implemented in an off-the-shelf RFID system.

All of the above anti-collision solutions [19-28] assume that application scenarios of RFID are stationary, and the wireless channel between a reader and tags is always in an ideal state, that is, without fully considering many challenges in actual situations, such as signal attenuation, tag or reader movement and multi-path effect, etc. However,

the instability nature of physical layer can seriously affect the multi-tag reading performance. Although some works [29-30] have been proposed for practice where the channel quality between the reader and tags changes over time and the signal suffers from problems such as path loss and signal attenuation, they do not solve the tags reading problem. Instead, they mainly focus on channels switching to adapt to channel quality and data rates in order to reduce packet loss rate and improve the overall network throughput.

Many works also [31-34] focus on the reading performance analysis of RFID anti-collision algorithms by using experimental verification. The literature [31] evaluates the reading performance of EPC C1 Gen2 RFID system in a realistic setting. The presented findings show that the physical layer effects are vital factors influencing the reading performance of a practical RFID system. The authors in [32] carry out extensive experiments on an industrial conveyor belt to study the impact of mobility on RFID reading performance. In [33], an iterative tag search protocol (ITSP) is presented to solve the specific tags search problem under the noisy channel. However, it fails to identify all tags within a specified time and is not compatible with EPC C1 Gen2 standard due to significant modification and high hardware cost requirements. The literature [34] explores the performance of cardinality estimation in a real RFID measuring scenario. Their findings indicate that the physical layer phenomena such as radio waves propagation and reception have a more significant impact on EPC C1 Gen2 reading performance.

Recent research work focus on parallel decoding techniques by modifying the EPC C1 Gen2 standard to improve time efficiency [35-38]. They try to recover collided tag signals based on specialized instruments like USRP. The authors in literature [35] implement a new solution namely BUZZ which enables rateless code transmission. Both LF-Backscatter [36] and BiGroup [37] use the separation of collided signals in the In-phase and Quadrature (IQ) domains to decode them. However, their performance relies on stable and distinct signals in time or IQ domain. To tackle the above challenges, FlipTracer [38] is proposed to achieve highly reliable parallel decoding by using observed transition probabilities between signals' combined states.

3 Preliminaries and System Model

The UHF RFID system consists of two communication data links: the forward link and reverse link. Among them, the communication link from the reader to tags is called the forward link, the communication link from tags to the reader is called the reverse link.

In the forward link, the reader sends continuous waves containing the command data to tags, each tag energizes itself by absorbing the RF energy through its antenna and converts such RF energy into a stable working voltage. Meanwhile, the demodulation circuit of tags recovers the baseband signal from carrier waves containing the modulated command data, and then a tag responds to the command when its digital baseband circuits finish the processing of reader's command. In the reverse link, a tag responds to the reader according to the received command by performing FM0 or Miller coding on the response data, adjusting the reflection coefficient of the tag antenna and implementing backscatter modulation.

In the UHF RFID system, the reader radiates electromagnetic field energy to the surrounding space through the antenna.The power density (also known as the Poynting vector) from the reader antenna d is [39]

$$S = \frac{P_{reader} G_{reader}}{4\pi d^2} \tag{1}$$

where P_{reader} and G_{reader} are the transmitted power and the antenna gain of the reader, respectively, and d is the distance between a reader and a tag. The effective area A_e of the tag antenna is defined as

$$A_e = \frac{\lambda^2}{4\pi} G_{tag} \tag{2}$$

where G_{tag} is antenna gain of a tag and λ is the wavelength of the carrier signal. According to (1) and (2), the energy received by a tag antenna at d meters away from the reader can be expressed by Friis formula

$$P_{tag} = S \cdot A_e = \frac{P_{reader} G_{reader} G_{tag} \lambda^2}{(4\pi d)^2} \tag{3}$$

The power received by a tag depends on the matching degree of its antenna impedance Z_A and the tag chip impedance Z_L. When Z_A and Z_L do not match exactly, some of the energy from the reader will be reflected by the tag antenna, the reflectance coefficient of incident wave Γ can be defined as

$$\Gamma = \frac{Z_A^* - Z_L}{Z_A^* + Z_L} \tag{4}$$

When Z_A and Z_L are conjugate matched, the tag chip receives the most power. According to radar technology, when the size of an object exceeds half of the electromagnetic wave, the electromagnetic wave will be reflected by the object. The reflection efficiency of the object is proportional to its Radar Cross Section (RCS) σ, which can be expressed as [40]

$$\sigma = p\Gamma^2 G_{tag}^2 \frac{\lambda^2}{4\pi} \tag{5}$$

where p is the polarization coefficient. The RCS of the tag σ and the power density S are proportional to the reflected power of the tag. According to (1) and (5), the reflected power of the tag $P_{tag,tx}$ can be expressed as

$$P_{tag,\,tx} = \sigma \cdot S = \frac{\sigma P_{reader} G_{reader}}{4\pi d^2} \tag{6}$$

Let χ_T denotes the backscatter coefficient of the tag, we have

$$\chi_T = \sigma / A_e \tag{7}$$

Then, the reflected power of the tag can be rewritten as

$$P_{tag,\,tx} = \frac{P_{reader} G_{reader} G_{tag} \lambda^2 \chi_T}{(4\pi d)^2} \tag{8}$$

The received power of the tag can be written as

$$P_{tag,\,rx} = \frac{P_{reader} G_{reader} G_{tag} \lambda^2 (1 - \chi_T)}{(4\pi d)^2} \tag{9}$$

According to the Friss formula, keeping d meters distance from the tag, the reflected p ower r eceived b y the reader in free space can be expressed as [41]

$$P_{reader,\,rx} = \frac{P_{tag,\,tx} G_{reader} G_{tag} \lambda^2 \chi_T}{(4\pi d)^2} = \frac{P_{reader} G_{reader}^2 G_{tag}^2 \lambda^4 \chi_T}{(4\pi d)^4} \quad (10)$$

From (9) and (10), the power received by the tag chip is inversely proportional to the square of the distance d when the reader's transmission power and carrier frequency are fixed, and the reflected power from the tag received by the reader is inversely proportional to fourth power of d. According to the specification of EPC C1 Gen2, in 860-960MHz band, the maximum effective radiated power of reader is 36 dBm. The antenna gain of a reader and a tag are 6 dBi and 2 dBi, respectively. It is assumed that the loss introduced by antenna polarization and matching is 3 dBi. From (9)-(10), the relationship between $P_{tag,\,rx}$, $P_{reader,\,rx}$ and d at the frequency of 915 MHz is shown in Fig. 2. At present, the receiving sensitivity of reader can reach -80 dBm, and its maximum working distance can reach 30 meters as illustrated in Fig. 1. Meanwhile, the maximum reading sensitivity of commercial tag is -22 dBm. The maximum working distance limited by reading sensitivity of the tag is 18 meters.

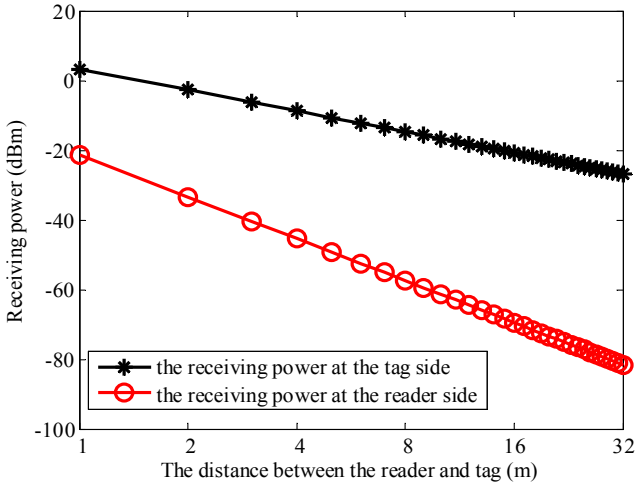

Fig. 1. Relationship between the receiving power and distance

Therefore, the reading performance of RFID system is highly related to the distance between the reader and tags. In a realistic scenario, the situation may be more complex due to multiple reflections from different objects, multi-path fading and shadowing, etc., which makes the signal attenuation occur with a certain probability. Thus, the propagation channel can be characterized by probabilistic modeling [42]. To identify a tag successfully in a UHF RFID system, there are two prerequisites. Firstly, the received power at tag side should be above the tag sensitivity ($P_{tag,\,rx} > P_{st}$). Secondly, the received power at reader side should be above the reader sensitivity ($P_{reader,\,rx} > P_{rt}$). The sensitivity of a tag or reader denotes its minimum working power.

4 Tag Identification Algorithm Under the Unreliable Channel

4.1 Probabilistic Identification Model Under a Mobile Environment

Since the signal attenuation is probabilistic occurred due to path loss, backscatter efficiency, multi-fading and capture effect, we can model the tag identification process by using the probabilistic model. We assume that the effective communication distance between the reader and tags is d. It is noted that the proposed propagation identification model is based on EPC C1 Gen2 standard. The link timing specified by EPC C1 Gen2 is illustrated in Fig. 2. The communication flows between the reader and tags under an ideal environment can be divided into four interactive phases.

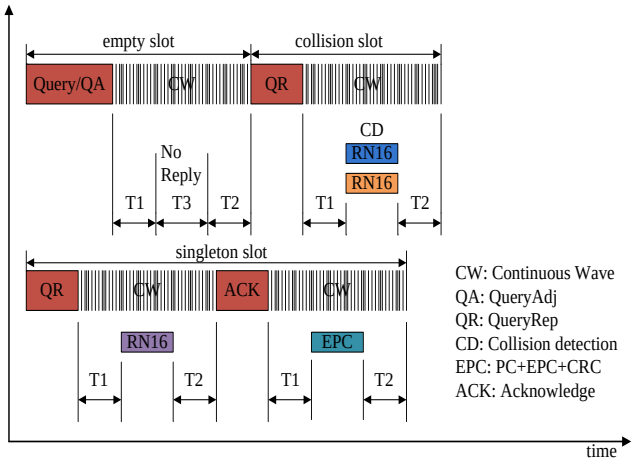

Fig. 2. The link timing in EPC C1 Gen2 RFID

1) The reader initializes an identification process by broadcasting a Query (which specifies the number of available slots F) command to the tags within the reader vicinity. Those tags that receive the Query command randomly select a time slot and load the index value of the slot into its slot counter (T_{sc}). A tag whose $T_{sc} = 0$ responds to the reader with a 16-bit random number (RN16).

2) The reader sends a QueryRep command to start a slot (The first slot of a frame is initialized by Query/QueryAdj command). Those tags receive the QueryRep command decrease its T_{sc}, and respond to the reader with RN16s when its $T_{sc} = 0$.

3) Only if the reader gets a correct RN16, it will send an Ack command containing the same RN16. The tag that receives the Ack command will check the RN16 field. If it matches its own, it responds with its ID.

4) After reading F slots, the reader updates a new frame length according to the slot statistics, and starts a new identification round by broadcasting a new Query or QueryAdj command.

In an ideal environment, as long as a tag is within the reader's coverage, the communication between the reader and the tag can be assumed perfect, i.e., unaffected by the channel quality. Suppose there are n tags within the reader coverage and the frame length F is used to identify them,

the probability that a given slot is an empty, singleton or collision can be calculated as

$$P_e = \left(1 - \frac{1}{F}\right)^n \tag{11}$$

$$P_s = \frac{n}{F} \cdot \left(1 - \frac{1}{F}\right)^n \tag{12}$$

$$P_c = 1 - P_e - P_s \tag{13}$$

However, consider a realistic propagation environment, the communication channel between the reader and tags is unreliable. Thus the occurrence probability of empty, singleton, and collision slot under the static RFID model will be changed. Fig. 3 illustrates a scenario of identifying moving tags under the unreliable channel and the corresponding slot status translation from an ideal channel to unreliable channel. In the following, we can derive the probability of an empty, collision, and a singleton slot under a mobile environment.

Consider the uncertainty of communication channel between the reader and tags, let $P_{trR} = \mathrm{Prob}\{P_{tag,\,rx} > P_{st}\}$ denote the probability that a tag can correctly receive the reader's command, $P_{Rrt} = \mathrm{Prob}\{P_{reader,\,rx} > P_{rt}\,|P_{tag,\,rx} > P_{st}\}$ denote the probability that the reader can correctly decode the tag's response.

Lemma 1. *Assume there are n tags waiting to be identified with an initialized frame length F, the number of responding tags in the frame is*

$$\widehat{n} = n \cdot (P_{trR})^2 \tag{14}$$

Proof: According to the interactive phases between the reader and tags described above, the tags firstly obtains the parameter F from the Query command with probability P_{trR}, the number of tags participating in the current phase can be expressed as

$$n^* = n \cdot P_{trR} \tag{15}$$

In the second phase, each participating tag randomly selects a time slot from F, and detects a QueryRep command to respond to the reader with its RN16s. Due to the loss of QueryRep command affected by the unreliable channel, the probability that a tag with $T_{sc} = x$ responds to the reader at y-th ($y \geq x$) slot can be written as

$$P_{tr}(F,\ x,\ y) = P_{trR} \cdot C_{y-1}^{x-1} (P_{trR})^{x-1} (1 - P_{trR})^{y-x} \tag{16}$$

Only when ($x \leq y \leq F$) is satisfied, a tag with $T_{sc} = x$ can respond to the reader within the current frame, i.e., during F slots, the corresponding probability can be expressed as

$$P_{tcr}(F,\ x,\ y) = \sum_{y=x}^{F} P_{tr}(F,\ x,\ y) \tag{17}$$

As the T_{sc} of the participating tags follow the uniform distribution, the probability that an arbitrary tag can respond to the reader at a slot within the current frame can be calculated as

$$P_{tr}^a(F,\ x,\ y) = \frac{1}{F} \sum_{x=1}^{F} \sum_{y=x}^{F} P_{tr}(F,\ x,\ y) \tag{18}$$

Since $1 \leq x \leq y \leq F$, the (18) can be rewritten as

$$\begin{aligned} P_{tr}^a(F,\ x,\ y) &= \tfrac{1}{F} \sum_{y=1}^{F} \sum_{x=1}^{y} P_{tr}(F,\ x,\ y) \\ &= \tfrac{1}{F} \sum_{y=1}^{F} P_{trR} \cdot \sum_{x=1}^{y} C_{y-1}^{x-1} (P_{trR})^{x-1} (1 - P_{trR})^{y-x} \\ &= \tfrac{1}{F} \sum_{y=1}^{F} P_{trR} \cdot (P_{trR} + 1 - P_{trR})^{y-1} = P_{trR} \end{aligned} \tag{19}$$

Thus, for an arbitrary tag, it can successfully respond to the reader in the current frame with the probability of P_{trR}. Therefore, the total number of tags successfully respond to the reader can be calculated as $\widehat{n} = n \cdot (P_{trR})^2$. □

Due to the uncertainty of communication channel, the slot distribution probability under the statistic RFID model will also be changed.

Lemma 2. *Assume there are n tags waiting to be identified with an initialized frame length F, the expected number of identified tags in the frame is*

$$\begin{aligned} E(N_s) = [F \cdot \sum_{m=2}^{\widehat{n}} P(m) \cdot m \cdot (1 - P_{Rrt})^{m-1} \\ + \widehat{n} \left(1 - \tfrac{1}{F}\right)^{\widehat{n}-1}] \cdot P_{trR} \cdot P_{Rrt}^2 \end{aligned} \tag{20}$$

Proof: Assuming that the original number of tags in a collision slot is m in the static RFID model, then the probability that they respond to the reader within a frame under the mobile model is

$$P(m) = \binom{\widehat{n}}{m} \left(\frac{1}{F}\right)^m \left(1 - \frac{1}{F}\right)^{\widehat{n}-m} \tag{21}$$

Hence, the probability that an empty, singleton, and multiple RN16 is successfully decoded by the reader can be recalculated as:

$$\begin{aligned} \hat{P}_e = \left(1 - \tfrac{1}{F}\right)^{\widehat{n}} + \tfrac{\widehat{n}}{F} \left(1 - \tfrac{1}{F}\right)^{\widehat{n}-1} (1 - P_{Rrt}) \\ + \sum_{m=2}^{\widehat{n}} P(m) \cdot (1 - P_{Rrt})^m \end{aligned} \tag{22}$$

$$\begin{aligned} \hat{P}_s = \tfrac{\widehat{n}}{F} \left(1 - \tfrac{1}{F}\right)^{\widehat{n}-1} \cdot P_{Rrt} \\ + \sum_{m=2}^{\widehat{n}} P(m) \cdot m \cdot (1 - P_{Rrt})^{m-1} \cdot P_{Rrt} \end{aligned} \tag{23}$$

$$\hat{P}_c = 1 - \hat{P}_e - \hat{P}_s \tag{24}$$

According to the interactive phases between the reader and tags, the expected number of identified tags can be derived as $E(N_s) = F \cdot \hat{P}_s \cdot P_{trR} \cdot P_{Rrt}$. □

If no capture effect occurs, the expected number of empty, singleton and collision slots can be calculated by using (22), (24) and the lemma 2. However, the capture effect commonly occurs when multiple tags simultaneously reply their data to the reader in EPC C1 Gen2 RFID system [43-44]. When the capture effect happens, more than one tags respond to the reader may produce a singleton slot. Let α denote the probability of capture effect, the expectation of

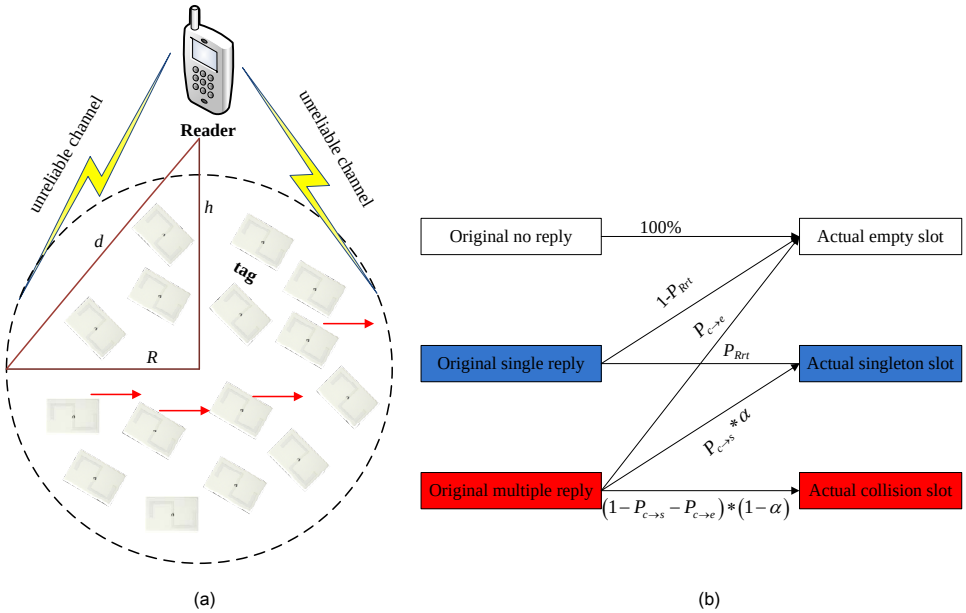

Fig. 3. The tags' reading scenarios in mobile environment

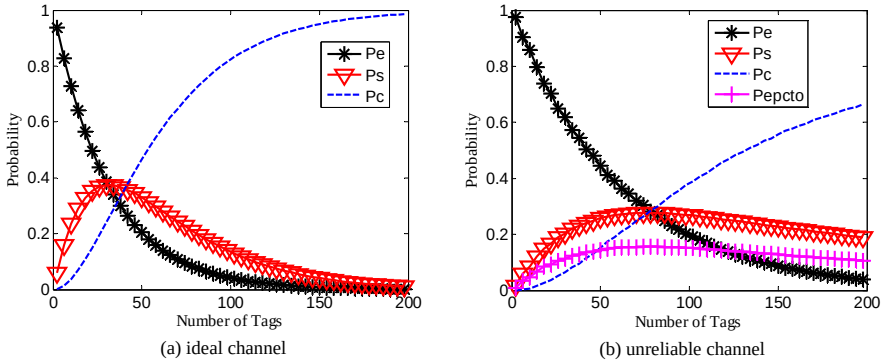

Fig. 4. The probability distribution of each slot type in ideal channel and unreliable channel

the number of empty slots (N_e), singleton slots (N_s) and collision slots (N_c) in a frame can be given as

$$E^*(N_e) = F \cdot \hat{P}_e \tag{25}$$

$$E^*(N_s) = F\left(\hat{P}_s + \alpha \cdot \hat{P}_c\right) \cdot P_{trR} \cdot P_{Rrt} \tag{26}$$

$$E^*(N_c) = (1-\alpha) \cdot F \cdot \hat{P}_c \tag{27}$$

According to (26), the slot efficiency under the dynamic environment can be expressed as

$$U = \left(\hat{P}_s + \alpha \cdot \hat{P}_c\right) \cdot P_{trR} \cdot P_{Rrt} \tag{28}$$

Fig. 4 compares the probability distribution of each slot type between ideal channel ($P_{trR} = P_{Rrt} = 1, \alpha = 0$) and unreliable channel ($P_{trR} = P_{Rrt} = 0.8$, $\alpha = 0.2$) when the number of tags is from 2 to 200, and an initial frame length is 32. P_e, P_s, and P_c are the probability of empty, success, and collision during a frame, respectively. Note that the P_s in Fig. 4 is equivalent to U. It can be seen that the unreliable channel will cause a sharp deterioration in slot efficiency. For example, as observed in Fig. 4 (a), the slot efficiency peaks at about 0.37 under the ideal channel. However, it drops sharply under unreliable channel as observed in Fig. 4 (b). Compared to slot types in Fig. 4 (a), there is a new slot type in Fig. 4 (b), namely EPC timeout slot (EPCTO), which means that the reader successfully transmits the Ack command but does not receive the tag's EPC. The expectation of the number of EPC timeout slots (N_{EPCTO}) can be written as

$$E(N_{EPCTO}) = F - E(N_e) - E(N_s) - E(N_c) \tag{29}$$

Because of the existence of such new slot type, the performance degradation caused by the unreliable channel cannot be avoided. It can also be observed in Fig. 4 (b), the upper bound of slot efficiency with conventional DFSA algorithm is 0.277. Under unreliable channel conditions, the relationship between an optimal frame length and corresponding range number of tags will also be changed. Therefore, it is necessary to design a novel anti-collision solution to improve the performance.

4.2 In-frame Cardinality Estimation

In order to achieve the best RFID anti-collision performance under dynamic environment, the number of tags n, P_{trR}, P_{Rrt}, and α should be estimated. According to (25), (26), and (27), the Minimum Squared Error (MSE) method can be used to estimate the number of tags, P_{trR}, P_{Rrt}, and α. Note that the path loss of the forward and reverse channels between two communication antennas are roughly identical [40, 45, 46, 47]. The reasons are as follows. Firstly, considering the short range communication nature of RFID, the time interval between forward and reverse channels can be viewed as symmetrical. Secondly, to avoid interference, the frequency deviation between different RFID tags is very small. Therefore, the influence of such frequency deviation on channels can also be ignored. In the following, we use $P_{trR} = P_{Rrt}$ to simplify the analysis and calculation. Then, we can estimates P_{trR}, α, and n as follows.

$$\left(\hat{n}_{est},\ \hat{P}_{trR},\ \hat{\alpha}\right) = \underset{n\in N,\ P_{trR},\ \alpha\in[0,\ 1]}{\arg\min} \left\|\mathbf{E}\left(\mathbf{n},\ \mathbf{P_{trR}},\ \alpha\right) - \mathbf{O}\right\|^2 \tag{30}$$

where $\|*\|$ is an Euclidean norm, $\mathbf{E}\left(\mathbf{n},\ \mathbf{P_{trR}},\ \alpha\right)$ is the expected values of empty slots, singleton slots and collision slots, $\mathbf{O}$ is the corresponding actual observation results by the reader. N denotes the search range of the number of tags. By using (30), the value of n, P_{trR}, and α can be estimated at the end of a frame. From (30), the proposed ECATI requires the 3-D searches for a minimum value of $\left\|\mathbf{E}\left(\mathbf{n},\ \mathbf{P_{trR}},\ \alpha\right) - \mathbf{O}\right\|^2$.

Let $U = |\hat{\alpha}|$, $V = \left|\hat{P}_{trR}\right|$, and $N = |\hat{n}_{est}|$, denote the cardinality of search space, w.r.t. the probability of capture effect, the probability of a tag can correctly receive the reader's command, and the number of tags, respectively. The number of brute searches required by the proposed ECATI is $U \cdot V \cdot N$. $\hat{n}^i_{est}$, $\hat{P}^i_{trR}$, and $\hat{\alpha}^i$ are the i-th searching value of n_{est}, P_{trR}, and α, respectively. Since (30) needs $U \cdot V \cdot N$ brute searches, ECATI's computational complexity can be expressed as

$$C^{\mathrm{ECATI}}_{cc} = O\left(U \sum_{j=1}^{V} \sum_{i=1}^{N} \hat{n}^i_{est} \times \hat{P}^j_{trR}\right) \tag{31}$$

Although the computational cost of ECATI is relatively high, it is not necessary to estimate the values of P_{trR} and α in real time in practical implementation. The reader can estimate them offline, that is, obtaining their values experimentally and then storing them in a look-up table. Consider a single reader and a tag, we can obtain the above parameters in the following way. We keep the tag at different distances d from the reader's antenna. And then we first set the frame length $F = 1$, and let the reader perform k rounds to read the same tag and record the number of successful reading k_1. Then we calculate the ratio $r_1 = k_1/k$. Secondly, we set the frame length F to a large value (e.g., $F = 128$), and also let the reader perform k rounds to read the same tag and record the number of successful reading k_2. Thus we calculate the ratio $r_2 = k_2/k$. Thirdly, consider a single reader and multiple tags, we set the frame length $F = 1$, and let the reader perform k rounds to read the a tag and record the number of successful reading k_3. Thus we calculate the ratio as $r_3 = k_3/k$.

According to the propagation model and the principle of the proposed ECATI, we can have

$$\begin{cases} r_1 = P^2_{trR} \cdot P^2_{Rrt} \\ r_2 = P^3_{trR} \cdot P^2_{Rrt} \\ r_3 = \alpha \cdot P^2_{trR} \cdot P^2_{Rrt} \end{cases} \tag{32}$$

Hence, the above environment parameters α, P_{trR}, and P_{Rrt} can be calculated as

$$\begin{cases} \alpha = \frac{r_3}{r_1} = \frac{k_3}{k_1} \\ P_{trR} = \frac{r_2}{r_1} = \frac{k_2}{k_1} \\ P_{Rrt} = \frac{k_1}{k_2}\sqrt{\frac{k_1}{k}} \end{cases} \tag{33}$$

We can store their values for various distance d. Therefore, the computational complexity of ECATI can be reduced and will not have a significant impact on the whole reading performance.

In addition, from Fig. 4, we know that the probability of empty is closing to zero when the number of tags is much greater than frame length. Under this scenario, $\left\|\mathbf{E}\left(\mathbf{n},\ \mathbf{P_{trR}},\ \alpha\right) - \mathbf{O}\right\|^2$ may not have a global minimum value. Let $\varepsilon = \left\|\mathbf{E}\left(\mathbf{n},\ \mathbf{P_{trR}},\ \alpha\right) - \mathbf{O}\right\|^2$, we plot a 3-D surface of ε for searching α and n. In Fig. 5, the frame length is initialized as 32, the number of tags is 200, $P_{trR} = 0.8$, and $\alpha = 0.2$. The observed results of $(N_e, N_s, N_c, N_{EPCTO})$ are (1, 4, 25, 2). As observed in Fig. 5, the canyon of the curve surface ε decreases monotonously with n. It is unable to obtain a global minimum value of ε. The above estimation function maybe difficult to be applied to large-scale tags identification when n is much greater than F due to the fact that P_e reaches zero. Moreover, it will also produce many collision slots and hence increase identification latency. In the following, we will introduce an estimation strategy to tackle such challenges. Consider an arbitrary slot in a frame F, the probability that the slot is an empty slot, singleton slot, collision slot and EPC time out slot can be calculated using (25)-(27), and (29). Specifically, a non-empty slot is either singleton , collision or EPC time out slot. For the first m non-empty slots, the number of EPC time out slots is $m - i - j$ if the number of singleton and collision slots is i and j, respectively. Then, the probability of i singleton slots, j collision slots and $m - i - j$ EPC time out slots can be expressed as

$$\begin{aligned} P_m = \sum_{i=0}^{m} \sum_{j=0}^{m-i} \binom{m}{i} \binom{m-i}{j} \left(\hat{P}_e\right)^i \\ \cdot \left((1-\alpha)\hat{P}_c\right)^j \left(P_{EPCTO}\right)^{m-i-j} \end{aligned} \tag{34}$$

where P_{EPCTO} can be expressed as $P_{EPCTO} = E\left(N_{EPCTO}\right)/F$. It is noted that (31) can be rewritten as $\left(1 - \hat{P}_e\right)^m$ by using multinomial theorem. So, P_m has nothing to do with α. Tab. 1 summarizes the theoretical and simulation values of P_m for $m = 1$ to 8 when $F = 128$ and the number of tags n varies from 100 to 1000. In each cell of the table, the numbers above are theoretical results, and the numbers in parentheses below are simulation results. In the simulations, the reader broadcasts a Query command and tags respond slot by slot. The theoretical results are derived from (31) and the simulation results are obtained by using Monte Carlo Simulations where the number of simulation

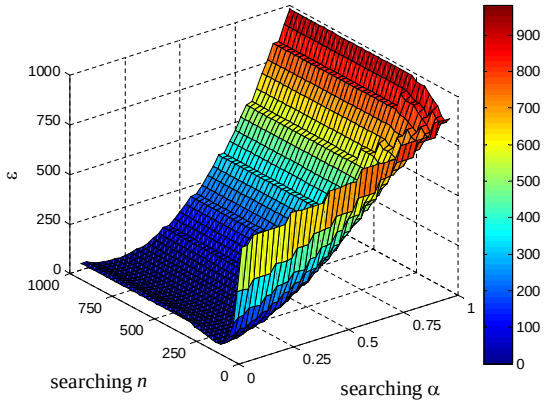

Fig. 5. 3D searching of number of tags and probability of capture effect with $n = 200$, $F = 32$

rounds is 250000. Observed from Tab. 1, regardless of the value of m, the P_m increases with the number of n. Especially, when $n = 1000$, P_m is very closed to 1. In other words, all of the first m slots in a frame are likely non-empty when the number of tags is much greater than frame length. Therefore, the frame length can be adjusted according to the observation statistics of the first m slots. The estimated cardinality can be given as

$$\hat{n}_{est} = \hat{n}^m_{est} \times \frac{F}{m} \tag{35}$$

where $\hat{n}^m_{est}$ is estimated results from the first m slots. Since the cardinality of search space, w.r.t the number of tags involved in the first m slots is relatively small, thus the computational overhead can be further reduced.

4.3 Optimal frame length

In a dynamic environment, the optimal frame length is also different from that in a static environment. Since the frame length setting affects the reading performance, an adaptive strategy is essential for the reader to set an appropriate frame length to achieve the optimal performance. We attempt to obtain a local optimal frame length for each identification round. The following theorem can be derived.

Theorem 1. *Assume there are n tags waiting to be identified, to maximize the slot efficiency within each frame, the local optimal frame length is*

$$F^* = \alpha + (1-\alpha) \cdot n \cdot (P_{trR})^2 \cdot P_{Rrt} \tag{36}$$

Proof: According to the interactive phases described in Section IV-A and Lemma 1, the number of tags involved in an identification round is calculated as $\widehat{n} = n \cdot (P_{trR})^2$. We denote these tags as a set S. Then due to the probabilistic propagation in the reverse link with a probability of P_{Rrt}, the number of slots that the reader can successfully decode an RN16 from a tag is $F \cdot \hat{P}_s$. For those tags in the set S, they randomly pick up time slots in a uniformly distributed manner and successfully return their RN16s with a probability of P_{Rrt}. We can further depict the above process as an equivalent model. That is, each tag in S randomly chooses a time slot from the frame with a probability of P_{Rrt} and responds with a probability of 100%. Base on such model, the number of tags involved in an identification round is

$$n_F = \widehat{n} \cdot P_{Rrt} \tag{37}$$

According to the analysis in previous works [8, 18, 21-24], for an ideal channel without capture effect, the local optimal frame length should be

$$F^* = n_F \tag{38}$$

By using the conclusion in [36-37], for a channel with capture effect, the local optimal frame length should be rewritten as

$$F^* = \alpha + (1-\alpha) \cdot n_F \tag{39}$$

Substituting (35) into (36), the local optimal frame length in the proposed propagation model can be expressed as

$$\begin{aligned} F^* &= \alpha + (1-\alpha) \cdot \widehat{n} \cdot P_{Rrt} \\ &= \alpha + (1-\alpha) \cdot n \cdot (P_{trR})^2 \cdot P_{Rrt} \end{aligned} \tag{40}$$

□

Based on the theorem 1, in each identification round, the reader can easily calculate F^* according to the current number of remaining tags n, the estimated P_{trR}, and α. Fig. 6 plots the slot efficiency under various frame length with $\alpha = 0.2$ and $P_{trR} = 0.8$. As depicted, it is clear that for an arbitrary set of values n, there is a local optimal frame length F for which the maximum slot efficiency can be obtained. Specifically, when $n = \frac{F-\alpha}{(1-\alpha)\cdot(P_{trR})^2 \cdot P_{Rrt}}$, the slot efficiency peaks at the highest point, which verifies the effectiveness of the theorem 1.

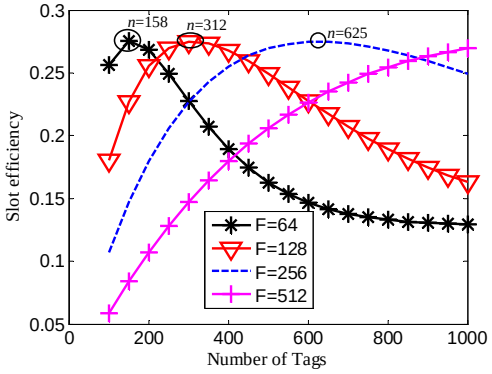

Fig. 6. Slot efficiency for different n and F with $\alpha = 0.2$ and $P_{trR} = 0.8$

5 Numerical Results

In this section, we evaluate the performance of ECATI algorithm in slot efficiency, time efficiency and energy efficiency, and compare it with state-of-the-art solutions including MAP [21], ILCM [24], EACAEA [23], SUBF-DFSA [26], and DS-MAP [28]. Simulations with a reader and various number of tags have been conducted using MATLAB, where the tags are uniformly distributed in the reader vicinity so that all tags can receive the reader's command. In our simulations, the number of tags is chosen between 100 to 1500. To reduce the randomness and ensure the convergence, the simulation results are averaged over 1000 iterations. The

TABLE 1
PROBABILITY THAT ALL OF THE FIRST m SLOTS ARE NON-EMPTY WHEN $F = 128$

n	$m=1$	$m=2$	$m=3$	$m=4$	$m=5$	$m=6$	$m=7$	$m=8$
100	0.3303 (0.3305)	0.1084 (0.1092)	0.0355 (0.0361)	0.0112 (0.0119)	0.0037 (0.0039)	0.0012 (0.0013)	0.0004 (0.0004)	0.0001 (0.0001)
200	0.5521 (0.5518)	0.3026 (0.3044)	0.1665 (0.1680)	0.0913 (0.0927)	0.0502 (0.0511)	0.0270 (0.0282)	0.0146 (0.0155)	0.0081 (0.0085)
400	0.7979 (0.7991)	0.6367 (0.6385)	0.5089 (0.5103)	0.4091 (0.4077)	0.3237 (0.3258)	0.2586 (0.2604)	0.2064 (0.2080)	0.1638 (0.1662)
800	0.9590 (0.9596)	0.9200 (0.9209)	0.8841 (0.8837)	0.8489 (0.8480)	0.8143 (0.8138)	0.7811 (0.7810)	0.7489 (0.7495)	0.7176 (0.7192)
1000	0.9817 (0.9819)	0.9641 (0.9641)	0.9465 (0.9467)	0.9293 (0.9295)	0.9127 (0.9127)	0.8958 (0.8962)	0.8799 (0.8800	0.8622 (0.8641)

TABLE 2
THE PARAMETERS USED IN MATLAB SIMULATIONS

Simulation scenario	A (low rate mode)	B (high rate mode)
R->T Modulation	PR-ASK	DSB-ASK
R->T coding	PIE	PIE
Tari (μs)	25	6.25
PW (μs)	12.5	3.13
RTcal (μs)	62.5	15.63
TRcal (μs)	85.33	20
DR	21.33	8
T->R Modulation	Miller-4	FM0
TREXt	1	1
BLF (kHz)	250	400
Data rate (kbps)	62.5	400
Simulation rounds	1000	1000
P_{trR}	0.8	0.7
α	0.2	0.3
P_{Rt} (mW)	825	825
P_{Rr} (mW)	125	125

parameter used in MATLAB simulations are listed in Tab. 2.

Fig. 7 compares slot efficiency, time efficiency and energy efficiency of various algorithms under Scenario A when the number of tags varies between 100 and 1500. The frame length is initialized as 64, $P_{trR} = P_{Rrt}$ and α are 0.8 and 0.2, respectively. As can be observed from Fig. 7 (a), the proposed ECATI can always maintain higher stability and slot efficiency. The reason is that the proposed estimation strategy can obtain the accurate estimation results of n_{est}, P_{trR}, and α, and can adjust an appropriate frame length corresponding to the unreliable channel condition. Time efficiency can better reflect the reading performance of the anti-collision algorithm considering the differences in duration between various types of time slots. The comparison of time efficiency of various algorithms is plotted in Fig. 7 (b). We can observe that, the performance ranking of algorithms from the highest to the lowest is ECATI, EACAEA, DS-MAP, SUBF-DFSA, ILCM and MAP, which is slightly different from the ranking in Fig. 7 (a). For example, the slot efficiency of ILCM is higher than that of SUBF-DFSA. However, its time efficiency is lower than SUBF-DFSA. Since the time efficiency considers the disparity in duration between different slot types, the advantages of the proposed ECATI is more obvious. The reason is that the number of empty slots is much greater than that of collision slots in ECATI, and the time duration of an empty slot is shorter than that of a collision slot. As an increasing number of handheld readers and tags deployed in IoT, energy consumption becomes a crucial issue. Fig. 7 (c) further compares the energy efficiency of various algorithms. The energy efficiency also highly depends on the time parameters and the distribution of slot type. As can be found, the proposed ECATI is the only algorithm that can maintain good performance in both slots, time and energy efficiency. Moreover, since our presented solution is based on EPC C1 Gen2 UHF RFID standard, it can be easier to implement in the off-the-shelf RFID reader.

Fig. 8 further compares the slot efficiency, time efficiency and energy efficiency of various algorithms under Scenario B when $P_{trR} = P_{Rrt} = 0.7$ and $\alpha = 0.3$. The frame length is also initialized as 64. The Scenario B is high rate mode ($data\ rate \geq 320$kbps). Intuitively, the higher the data rate, the greater the performance can be achieved. However, as can be observed in Fig. 8 (a), the slot efficiency of all algorithms deteriorates under scenario B. The reason is that as the channel conditions deteriorate, the number of tags that can be successfully identified in a frame drop dramatically, causing sharp slot efficiency degradation. For example, the SUBF-DFSA derives the probability relationship between the collision slot and empty slot based on the ideal channel. However, such a relationship will no longer be applied under unreliable channel conditions, resulting in slot efficiency degradation. The lower the P_{trR}, the performance degradation becomes more obvious. Therefore, as observed in Fig. 8 (a), the slot efficiency of SUBF-DFSA is lowest. Fig. 8 (b) and Fig. 8 (c) plot the time efficiency and energy efficiency of various algorithms, respectively, which shows similar results. Different from the conventional DSFA solutions, the proposed ECATI can estimate the P_{trR} and α, weakening the negative effects they can bring. Furthermore, the proposed ECATI can effectively resist the tag misreading compared to other solutions. So, it can identify more tags at a given time interval. Also, the number of empty slots consumed by ECATI is much greater than the number of collision slots. Benefit from these two aspects, the proposed ECATI can achieve the best slot efficiency, time efficiency, and energy efficiency under unreliable channel conditions.

Fig. 9 compares the misreading ratio of various algorithms when the number of tags is from 5 to 100. The frame length is initialized as 16. In Fig. 9 (a), $P_{trR} = 0.8$ and $\alpha = 0.2$, and the data rate is 62.5 kbps. As can be observed, the performance of conventional anti-collision algorithms is greatly affected by channel conditions, especially when the number of tags is rather small. For example, when the number of tags to be identified is 5, the number of missed

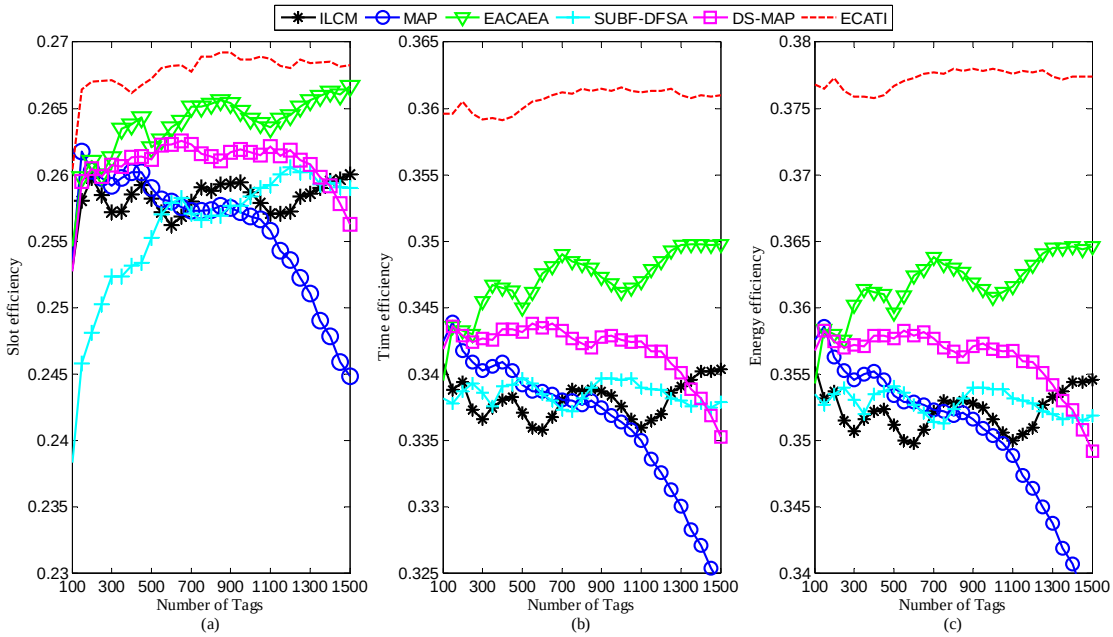

Fig. 7. Comparison of various performance metrics under Scenario A: (a) slot efficiency (b) time efficiency (c) energy efficiency

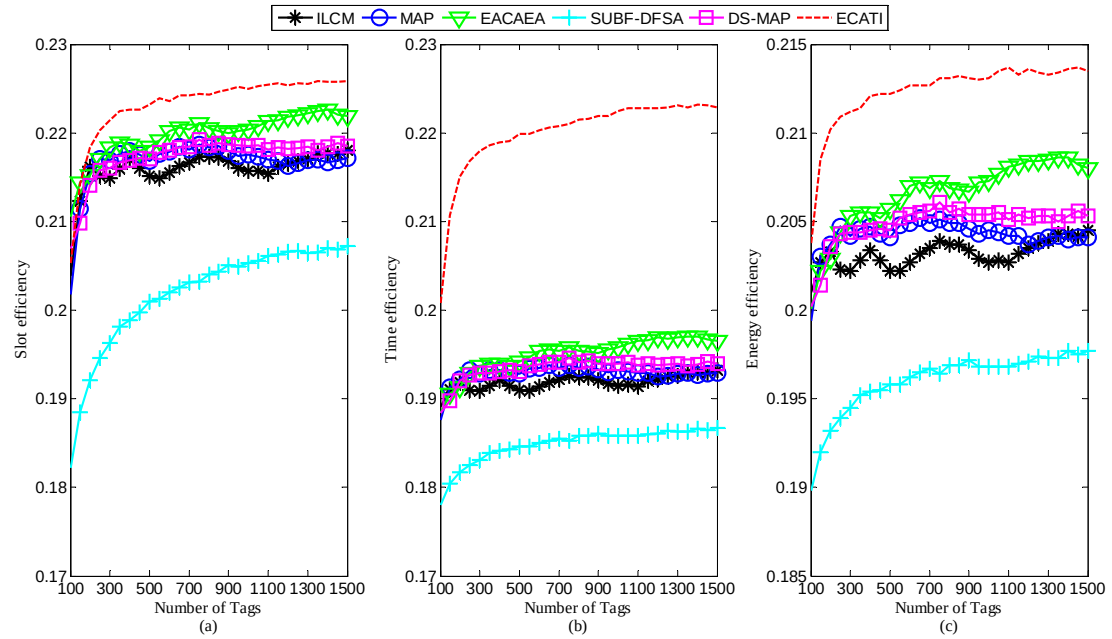

Fig. 8. Comparison of various performance metrics under Scenario B: (a) slot efficiency (b) time efficiency (c) energy efficiency

reading tags expended by EACAEA is 1. Thus the missing ratio is 80%. As the number of tags increases, the absolute number of miss reading tags will be reduced, thus leading to a decreased missing ratio. Since conventional DFSA algorithms estimate the remaining tags by using the number of empty slots, success slots and collision slots, they are unable to avoid the misreading problem when the shared channel is unreliable. As a contrary, the proposed ECATI can completely identify the whole tag set. In an ideal channel, the higher the data rates, the better the reading performance can be achieved. However, the reading performance is more related to channel quality rather than the data rate. As can be seen from Fig. 9 (b) in which $P_{trR} = 0.7$ and $\alpha = 0.3$, and the data rate is 400 kbps, the reading performance of all algorithms is worse than that of Fig. 9 (a). Benefiting from the estimation phase in a mobile environment, the proposed ECATI can maintain the best performance regardless of channel conditions.

6 Experimental Results With a Practical RFID Testbed

To further evaluate the performance of the proposed ECATI algorithm in a practical RFID scenario, we conduct experiments using an off-the-shelf RFID reader in a dynamic envi-

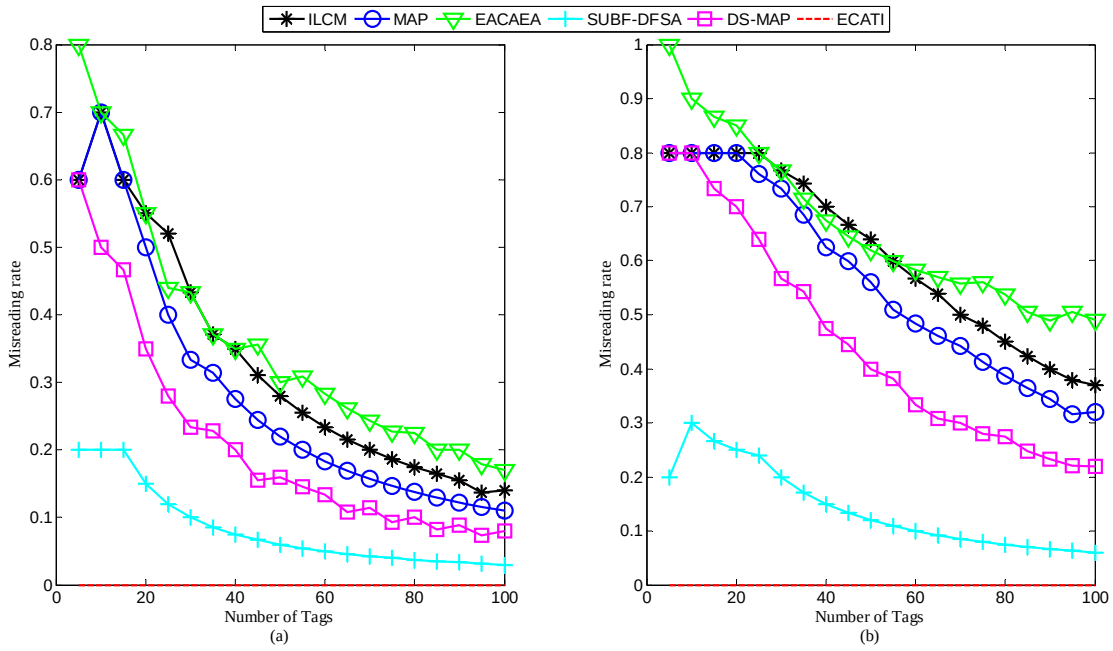

Fig. 9. Comparison of misreading ratio: (a) under Scenario A (b) under Scenario B

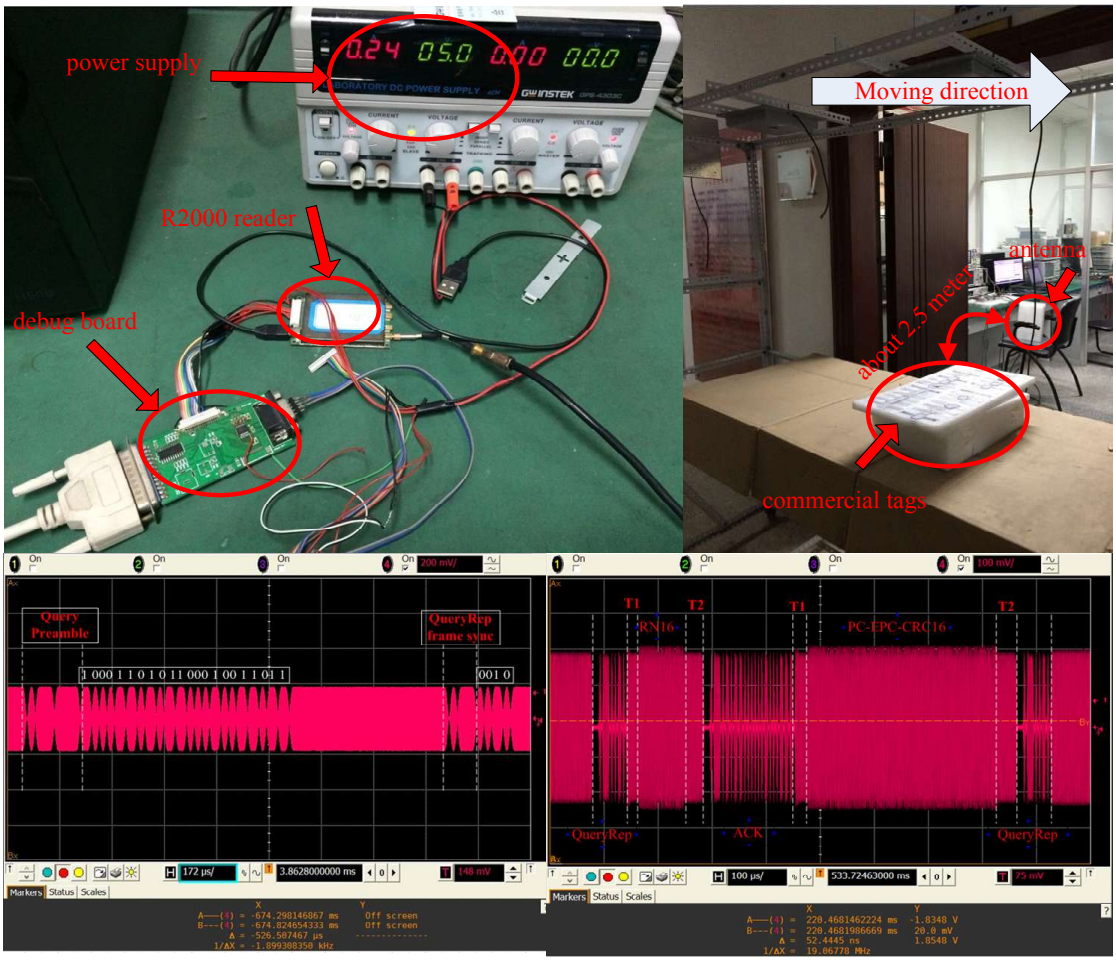

Fig. 10. The entire hardware setup of the experiments

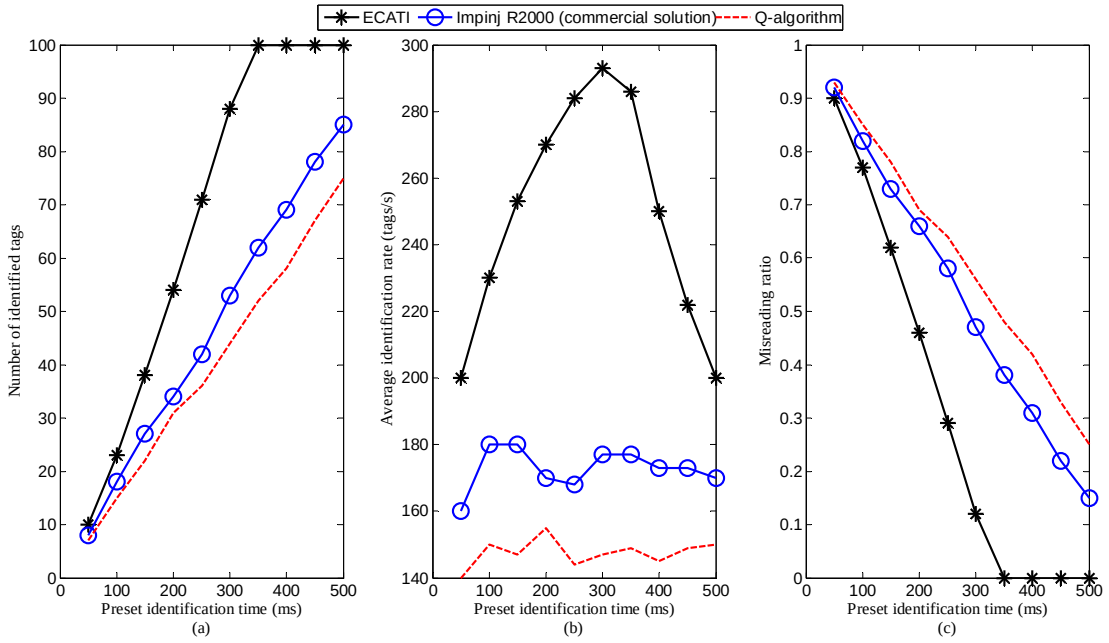

Fig. 11. Comparison of the experimental results: (a) the number of identified tags (b) average identification rate (c) misreading ratio

ronment. Experiments include an active commercial reader manufactured by Impinj and commercial tags equipped by Alien. The reader is equipped with AT91SAM7S256 microprocessor and Indy R2000 RF transceiver chip where AT91SAM7S256 is a 32-bit RISC microprocessor based on the ARM7TDMI core. The single-cycle access frequency is 30MHz, with 256KB flash memory size and 64KB SRAM memory size on the chip. The Indy R2000 reader chip integrates RF and baseband modules to receive data from compatible RFID tags, and is now widely used by industry and enterprise. For the convenience of description, the R2000 reader composed of AT91SAM7S256 microprocessor and Indy R2000 chip as core modules and the anti-collision solution provided by Impinj Inc itself is named as Impinj R2000 algorithm. The entire hardware environment used for experiments is captured in Fig. 10, which includes an R2000 reader, a debug board, power supply, an antenna and 100 commercial tags. During the practical experimental test, the tags are placed on a small trolley. The trolley can move out of the coverage of the reader. Because the test scenario has wall occlusion and mobility, the signal transmission between the reader and tags can be viewed as NLOS. Before the test of the anti-collision algorithms, we first capture the waveform through the oscilloscope to verify the function of the reader in order to detect the response from a tag, the detailed waveform is also illustrated in Fig. 10. Tab. 3 lists the link parameters configured for radio frequency communication between the reader and tags.

Fig. 11 compares the experimental results by using Q-algorithm, Impinj algorithm and the proposed ECATI algorithm to identify the same batch tags within the same time period under the given RF link parameters. The experiments are carried out by placing commercial tags about 2.5 meters away from the reader's antenna with a fixed transmitting power. In order to better simulate the mobile scenario, we let the tag-loaded shelves move at a speed of 0.5 meters per second. And then, we evaluate and compare the reading performance of the standard Q-algorithm widely used in EPC C1 Gen2, the commercial solution Impinj and the proposed ECATI. To ensure the validity and reliability of the experimental results, we repeat 50 times for each experiment and then average them. Two commercial used metrics have been taken into account to compare practical performance of algorithms, that is, the number of identified tags at a given time interval and average identification rate.

TABLE 3
LINK PARAMETERS USED FOR RF COMMUNICATIONS

Parameters	Value
Carrier Frequency (MHz)	922.75
BLF (kHz)	400
Data-rate (kbps)	400
Modulation	DSB-ASK
Deviation (Hz)	20
Channel width (kHz)	250
RTcal (μs)	15.63
TRcal (μs)	20
DR	8
T->R modulation	FM0
Tari	6.25
TRExt	1

As can be observed from Fig. 11 (a), the proposed ECATI algorithm can identify more tags in a certain period. As the preset reading time increases, the performance advantages of the ECATI become more apparent. For example, when the reading time is set to 350 milliseconds (ms), the proposed ECATI can identify all 100 tags, whereas the Impinj R2000 and Q-algorithm can only identify 62 and 52 tags, respectively. As illustrated in Fig. 11 (b), the proposed ECATI improves the average identification rate (which is defined as the number of tags to be successfully identified per second) by 43.4% compared to Impinj R2000. Since no more remaining tags need to be identified when the reading time is

longer than 350 ms, the instantaneous average identification rate of ECATI will decrease sharply. The misreading ratio of various algorithms over time can also be observed in Fig. 11 (c). Since the ECATI can estimate the probabilistic parameters including P_{trR}, P_{Rrt} and α, it can better resist the harsh channel quality and thus improve the reading performance. Both simulation and experiment results verify the effectiveness of the proposed ECATI which outperforms the commercial solution equipped by Impinj in the practical RFID system.

7 Conclusion

In this paper, we have focused on the reading performance of DFSA algorithm for RFID tags identification under a mobile scenario, and a novel DFSA-based anti-collision strategy namely ECATI has been proposed for EPC C1 Gen2. Unlike conventional DFSA methods in stationary scenarios, the ECATI can accurately estimate the environment parameters including the probability of successful communication between readers and tags and the probability that a capture effect occurs, and hence optimize the identification process. Benefit from such estimation and optimization, the ECATI has been shown to improve the reading performance without significant extra hardware costs. The simulation results have also demonstrated that the ECATI outperforms the existing state-of-the-art DFSA solutions in terms of slot efficiency, time efficiency and energy efficiency. The experimental results have also been supplemented to verify the effectiveness of the proposed solution in practical mobile scenarios.

References

[1] A. J. Jara, M. A. Zamora, and A. F. G. Skarmeta, "An internet of things–based personal device for diabetes therapy management in ambient assisted living (AAL)," *Pers. Ubiquit. Comput.*, vol. 15, no. 4, pp. 431-440, 2011.

[2] A. Al.-Fuqaha, M. Guizani, M. Mohammadi, M. Aledhari, and M. Syyash, "Internet of things: A survey on enabling technologies, protocols, and applications," *IEEE Commun. Surveys Tuts.*, vol. 17, no. 4, pp. 2347-2376, 2015.

[3] X. Liu, K. Li, A. X. Liu, S. Guo, M. Shahzad, A. L. Wang, and J. Wu, "Multi-category RFID estimation," *IEEE/ACM Trans. Netw.*, vol. 25, no. 1, pp. 264-277, 2017.

[4] P. Yang, W. Wu, M. Moniri, and C. C. Chibelushi, "Efficient object localization using sparsely distributed passive RFID tags," *IEEE Trans. Ind. Electron.*, vol. 60, no. 12, pp. 5914-5924, 2013.

[5] K. Bu, M. Xu, X. Liu, J. Luo, S. Zhang, and M. Weng, "Deterministic detection of cloning attacks for anonymous RFID systems," *IEEE Trans. Ind. Informat.*, vol. 11, no. 6, pp. 1255-1266, 2015.

[6] C. Floerkemeier, "Transmission control scheme for fast RFID object identification," *Proc. 4th Annu. IEEE Int. Conf. Pervasive Comput. Workshops*, 2006, pp. 457-462.

[7] M. Kodialam and T. Nandagopal, "Fast and reliable estimation schemes in RFID systems," *Proc. 12th Annu. Int. Conf. Mobile comput. Netw.*, 2006, pp. 322-333.

[8] Y. He and X. Wang, "An ALOHA-based improved anti-collision algorithm for RFID systems," *IEEE Wireless Commun.*, vol. 20, no. 5, pp. 152-158, 2013.

[9] Y. Maguire and R. Pappu, "An optimal Q-algorithm for the ISO 18000-6C RFID protocol," *IEEE Trans. Autom. Sci. Eng.*, vol. 6, no. 1, pp. 16-24, 2009.

[10] L. Zhang, W. Xiang, X. Tang, Q. Li, Q. Yan, "A Time-and Energy-Aware Collision Tree Protocol for Efficient Large-Scale RFID Tag Identification," *IEEE Trans. Ind. Informat.*, vol. 14, no. 6, pp. 2406-2417, 2018.

[11] J. Su, Z. Sheng, G. Wen, and V. C.M. Leung, "A time efficient tag identification algorithm using dual prefix probe scheme (DPPS)," *IEEE Signal Process. Lett.*, vol. 23, no. 3, pp. 386-389, 2016.

[12] L. Zhang, W. Xiang, and X. Tang, "An efficient bit-detecting protocol for continuous tag recognition in mobile RFID systems," *IEEE Trans. Mobile Comput.*, vol. 17, no. 3, pp. 503-516, 2018.

[13] J. Myung, W. Lee, J. Jaideep, T. K. Shih, "Tag-splitting: adaptive collision arbitration protocols for RFID tag identification," *IEEE Trans. Parallel Distrib. Syst.*, vol. 18, no. 6, pp. 763-775, 2007.

[14] H. Guo, V. C.M. Leung, and M. Bolic, "M-Ary RFID tags splitting with small idle slots," *IEEE Trans. Autom. Sci. Eng.*, vol. 9, no. 1, pp. 177-181, 2012.

[15] M. Buettner and D. Wetherall, "An empirical study of UHF RFID performance," *Proc. 14th ACM Int. Conf. Mobile Comput. Netw. (Mobicom)*, 2008, pp. 223-234.

[16] S. R. Aroor and D. D. Deavours, "Evaluation of the state of passive UHF RFID: An experimental approach," *IEEE Syst. J.*, vol. 1, no. 2, pp. 168-176, 2007.

[17] J. Su, Z. Sheng, L. Xie, G. Li, and A. X. Liu, "Fast splitting based tag identification algorithm for anti-collision in UHF RFID system," *IEEE Trans. Commun.*, 2018, pp. 1-12, doi: 10.1109/TCOM-M.2018.2884001.

[18] L. Barletta, F. Borgonovo, and M. Cesana, "A formal proof of the optimal frame setting for dynamic-frame Aloha with known population size," *IEEE Trans. Inf. Theory*, vol. 60, no. 11, pp. 7221-7230, 2014.

[19] B. Knerr, M. Holzer, C. Angerer, and M. Rupp, "Slot-wise maximum likelihood estimation of the tag population size in FSA protocols," *IEEE Trans. Commun.*, vol. 58, no. 2, pp. 578-585, 2010.

[20] H. Wu and Y. Zeng, "Bayesian tag estimate and optimal frame length for anti-collision aloha RFID system," *IEEE Trans. Autom. Sci. Eng.*, vol. 7, no. 4, pp. 963-969, 2010.

[21] W.T-Chen, "An accurate tag estimate method for improving the performance of an RFID anticollision algorithm based on dynamic frame length ALOHA," *IEEE Trans. Autom. Sci. Eng.*, vol. 6, no. 1, pp. 9-15, 2009.

[22] J. V-Alonso, V. B-Delgado, E. E-Lopez, F. J. G-Castaño, and J. Alcaraz, "Multiframe maximum-likelihood tag estimation for RFID anticollision protocols," *IEEE Trans. Ind. Informat.*, vol. 7, no. 3, pp. 487-496, 2011.

[23] W. T-Chen, "Optimal frame length analysis and an efficient anti-collision algorithm with early adjustment of frame length for RFID systems," *IEEE Trans. Veh. Technol.*, vol. 65, no. 5, pp. 3342-3348, 2016.

[24] P. Šolić, J. Radić, N. Rožić, "Energy efficient tag estimation method for aloha-based RFID systems," *IEEE Sensors J.*, vol. 14, no. 10, pp. 3637-3647, 2014.

[25] L. Arjona, H. Landaluce, A. Perallos, and E. Onieva, "Timing-aware RFID anti-Collision protocol to increase the tag identification rate," *IEEE Access*, vol. 6, pp. 33529-33541, 2018.

[26] J. Su, Z. Sheng, D. Hong, and V. C.M. Leung, "An efficient subframe based tag identification algorithm for UHF RFID systems," *Proc. Int. Conf. Commun.(ICC 2016)*, 2016, pp. 1-6.

[27] J. Su, Z. Sheng, D. Hong, and G. Wen, "An effective frame breaking policy for dynamic framed slotted Aloha in RFID," *IEEE Commun. Lett.*, vol. 20, no. 4, pp. 692-695, 2016.

[28] Y. Chen, J. Su, and W. Yi, "An efficient and easy-to-implement tag identification algorithm for UHF RFID systems," *IEEE Commun. Lett.*, vol. 21, no. 7, pp. 1509-1512, 2017.

[29] P. Zhang, J. Gummeson, and D. Ganesan, "BLINK: A high throughput link layer for backscatter communication," in *Proc. ACM Mobisys*, 2012, pp. 99-112.

[30] W. Gong, H. Liu, K. Liu, Q. Ma, and Y. Liu, "Exploiting Channel Diversity for Rate Adaptation in Backscatter Communication Networks," in *Proc. INFOCOM*, 2016, pp. 1-9.

[31] L. Xie, Q. Li, X. Chen, S. Lu, and D. Chen, "Continuous Scanning with Mobile Reader in RFID Systems: an Experimental Study," *Proc. 14th ACM Int. Symp. on Mobile Ad Hoc Networking and Computing (MobiHoc)*, 2013, pp. 11-20.

[32] Z. Ren, C. C. Tan, D. Wang, and Q. Li, "Experimental study on mobile RFID performance," *Proc. Int. Conf. Wireless Algorithms Syst. Appl. (WASA 2009)*, 2009, pp. 12-21.

[33] M. Chen, W. Luo, Z. Mo, S. Chen, and Y. Fang, "An efficient tag search protocol in large-scale RFID systems with noisy channel," *IEEE/ACM Trans. Netw.*, vol. 24, no. 2, pp. 703-716, 2016.

[34] P. Šolić, J. Maras, J. Radić, and Z. Blažević, "Comparing theoretical and experimental results in Gen2 RFID throughput," *IEEE Trans. Autom. Sci. Eng.*, vol. 14, no. 1, pp. 349-357, 2017.
[35] J. Wang, H. Hassanieh, D. Katabi, and P. Indyk, "Efficient and reliable low-power backscatter networks," in *Proc. ACM SIGCOMM*, 2012, pp. 61-72.
[36] P. Hu, P. Zhang, and D. Ganesan, "Laissez-faire: Fully asymmetric backscatter communication," in *Proc. ACM SIGCOMM Comput. Commun. Rev.*, vol. 45, no. 4, pp. 255-267, 2015.
[37] J. Ou, M. Li, and Y. Zheng, "Come and be served: Parallel decoding for COTS RFID Tags," in *Proc. MOBICOM*, 2015, pp. 500-511.
[38] M. Jin, Y. He, X. Meng, Y. Zheng, D. Fang, and X. Chen, "FlipTracer: Practical parallel decoding for backscatter communication," in *IEEE/ACM Trans. Netw.*, vol. 27, no. 1, pp. 330-343, 2019.
[39] J. D. Kraus and R. J. Marhefka, "Antennas for all applications," *New York: McGraw-Hill*, 2002.
[40] P. V. Nikitin and K. V. S. Rao, "Antennas and propagation in UHF RFID systems," *Proc. 2008 IEEE Int. Conf. RFID*, 2008, pp. 277-288.
[41] M. O White, "Radar cross-section: measurement, prediction and control," *Electron. Commun. Eng. J.*, vol. 10, no. 4, pp. 169-180, 1998.
[42] L. Xie, B. Sheng, C. C. Tan, H. Han, Q. Li, and D. Chen, "Efficient tag identification in mobile RFID systems," *Proc. 29th Annu. Joint Conf. of the IEEE Computer and Commun. (INFOCOM 2010)*, 2010, pp. 1-9.
[43] B. Li and J. Wang, "Efficient anti-collision algorithm utilizing the capture effect for ISO 18000-6C RFID protocol," *IEEE Commun. Lett.*, vol. 15, no. 3, pp. 352-354, 2011.
[44] H. Wu and Y. Zeng, "Passive RFID tag anticollision algorithm for capture effect," *IEEE Sensors J.*, vol. 15, no. 1, pp. 218-226, 2015.
[45] W. Xu, X. Dong, and W. Lu, "Passive RFID tag anticollision algorithm for capture effect," *IEEE Trans. Commun.*, vol. 59, no. 5, pp. 1228-1235, 2011.
[46] C. He, S. Chen, H. Luan, X. Chen, and Z. Wang, "Monostatic MIMO backscatter communications," *IEEE J. Sel. Areas Commun.*, pp. 1-14, 2020, doi: 10.1109/JSAC.2020.3000823.
[47] J. Griffin and G. Durgin, "Complete link budgets for backscatter-radio and RFID systems," *IEEE Trans. Antennas Propag.*, vol. 51, no. 2, pp. 11-25, 2009.

Jian Su has been a lecturer in the School of Computer and Software at the Nanjing University of Information Science and Technology since 2017. He received his PhD with distinction in communication and information systems at University of Electronic Science and Technology of China (UESTC) in 2016. He holds a B.S. in Electronic and information engineering from Hankou university and an M.S. in electronic circuit and system from Central China Normal University. His current research interests cover Internet of Things, RFID, and Wireless sensors networking.

Zhengguo Sheng has been a senior lecturer in the Department of Engineering and Design at the University of Sussex since 2015. He received his Ph.D. and M.S. with distinction at Imperial College London in 2011 and 2007, respectively, and his B.Sc. from the University of Electronic Science and Technology of China (UESTC) in 2006. His current research interests cover the Internet of Things (IoT), connected vehicles, and cloud/ edge computing.

Alex X. Liu received his Ph.D. degree in Computer Science from The University of Texas at Austin in 2006, and is a professor at the Department of Computer Science and Engineering, Michigan State University. He received the IEEE & IFIP William C. Carter Award in 2004, a National Science Foundation CAREER award in 2009, and the Michigan State University Withrow Distinguished Scholar Award in 2011. He has served as an Editor for IEEE/ACM Transactions on Networking, and he is currently an Associate Editor for IEEE Transactions on Dependable and Secure Computing and IEEE Transactions on Mobile Computing, and an Area Editor for Computer Communications. He has served as the TPC Co-Chair for ICNP 2014 and IFIP Networking 2019. He received Best Paper Awards from ICNP-2012, SRDS-2012, and LISA-2010. His research interests focus on networking and security. He is a Fellow of the IEEE.

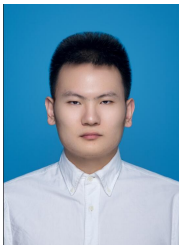

Yu Han received the B.S. degree from University of Electronic Science and Technology of China (UESTC), Chendu, China , in 2013, where he is currently pursing the Ph.D degree. His current research focuses on Energy Harvesting Wireless Sensor Networks and Backscatter Communication.

Yongrui Chen is currently an Associate Professor with the School of Electronic, Electrical and Communication Engineering, University of Chinese Academy of Sciences. He has received his M.S degree from Tsinghua University, China in 2007, and Ph.D. degree from University of Chinese Academy of Sciences, China in 2011. His research interests include Internet of Things, wireless and mobile computing, and heterogeneous wireless networks. He is an member of IEEE.